Title

Design and simulation of 4H-SiC low gain avalanche diode

Authors

Yang, Tao

Fu, Chenxi

Song, Weimin

et al.

Publication Date

2023-11-01

DOI

10.1016/j.nima.2023.168677

Nuclear Instruments and Methods in Physics Research A 1056 (2023) 168677

Contents lists available at ScienceDirect

Nuclear Inst. and Methods in Physics Research, A

journal homepage: www.elsevier.com/locate/nima

Full Length Article

Design and simulation of 4H-SiC low gain avalanche diode

Tao Yang [a,c], Chenxi Fu [d], Weimin Song [d], Yuhang Tan [e], Suyu Xiao [f], Congcong Wang [a,b], Kai Liu [g,h], Xiyuan Zhang [a,b], Xin Shi [a,b,*]

[a] Institute of High Energy Physics, Chinese Academy of Sciences, 19B Yuquan Road, Shijingshan District, Beijing 100049, China
[b] State Key Laboratory of Particle Detection and Electronics, 19B Yuquan Road, Shijingshan District, Beijing 100049, China
[c] University of Chinese Academy of Sciences, 19A Yuquan Road, Shijingshan District, Beijing 100049, China
[d] College of Physics, Jilin University, 2699 Qianjin Avenue, Chaoyang District, Changchun 130015, China
[e] Research Center for Medical Artificial Intelligence, Shenzhen Institute of Advanced Technology, Chinese Academy of Sciences, 1068 Xueyuan Avenue, Shenzhen University Town, Shenzhen 518055, China
[f] Shandong Institute of Advanced Technology, 100 Fanlong Road, Jinan 250103, China
[g] School of Nuclear Science and Technology, Lanzhou University, 222 Tianshui Road(South), Chengguan District, Lanzhou 730000, China
[h] Frontiers Science Center for Rare Isotopes, and Lanzhou Center for Theoretical Physics, Lanzhou University, 222 Tianshui Road(South), Chengguan District, Lanzhou 730000, China

ARTICLE INFO

Keywords:
LGAD
4H-siC
Semiconductor particle detector
TCAD

ABSTRACT

In the applications of nuclear and high-energy physics, Silicon Low Gain Avalanche Diodes (Si LGAD) as particle detectors have been shown to perform well in time resolution. Compared with silicon, 4H Silicon Carbide (4H-SiC) has a wider band gap, better radiation resistance, higher saturated carrier velocity and lower temperature sensitivity. Therefore, 4H-SiC LGAD is suitable for the detection of Minimum Ionization Particles (MIPs) under extreme radiation and temperature. However, due to the complexity of SiC device design and production, high performance SiC LGAD devices have not yet been produced. In this work, we use TCAD tools to design and simulate two n-type 4H-SiC LGAD structures with different electric field profiles, I/V and C/V characteristics and gain efficiencies. Through the analysis of simulation results, the LGAD with a triangle electric field profile in the gain layer has a higher gain efficiency, while the design with a trapezoid electric field profile is less affected by the gain layer thickness and more stable at high temperature. Subsequently, we will develop a set of SiC production processes under the guidance of this work.

1. Introduction

In the past decade, the search for 4D (resolvable both in time and space) detectors with high radiation hardness and robustness are one of the major challenges in experimental high-energy physics. The detectors will be applied to particle colliders and nuclear reactors with internal irradiation flux exceeding 2×10^{16} n_{eq}/cm^2 [1]. Timing performance, as one of the most valuable qualities for 4D detectors, is strongly dependent on the carrier drifting velocity and signal noise ratio (S/N) [2]. In the past few years, various groups have developed and verified that the time resolution of Silicon LGAD is better than 50 ps because of its good S/N in the low gain range (10–100) [3–11]. However, when the irradiation fluence increases to 2.5×10^{15} n_{eq}/cm^2, the number of collected charges of Silicon LGAD will decrease significantly, making it difficult to keep high performance under such a high irradiation environment. Moreover, Silicon LGAD must be cooled to −30 °C to compensate for the rapidly increasing leakage current under extreme irradiation conditions, which undoubtedly increases the manufacturing cost of large particle detectors [11–13]. In this situation, the continuous improvement of the radiation resistance of Silicon LGAD could reach the physical boundary of Si materials. Therefore, developing a new solution of novel material is another way forward to adapt to MIPs detection in a high irradiation environment.

As a wide band-gap semiconductor, Silicon Carbide (SiC) has excellent intrinsic characteristics to fabricate radiation-resistant devices. Benefiting from the fast development of the industrial investment of SiC power electronic devices, and the fabrication process on SiC substrate, it is now possible to utilize SiC detectors in environments characterized by high irradiation flux and high temperature. Among the main SiC polytypes (3C, 4H and 6H), 4H-SiC has the highest band-gap (3.26 eV), which means that its potential radiation hardness is the highest [14] and it is the most concerned material in the study of high radiation hardness. Compared to Silicon, 4H-SiC has higher atomic displacement energy, higher saturated velocity and is more stable at high temperatures. Therefore, a 4H-SiC device would have a faster time response

* Corresponding author at: Institute of High Energy Physics, Chinese Academy of Sciences, 19B Yuquan Road, Shijingshan District, Beijing 100049, China.
E-mail addresses: zhangxiyuan@ihep.ac.cn (X. Zhang), shixin@ihep.ac.cn (X. Shi).

https://doi.org/10.1016/j.nima.2023.168677
Received 16 November 2022; Received in revised form 21 August 2023; Accepted 8 September 2023
Available online 18 September 2023

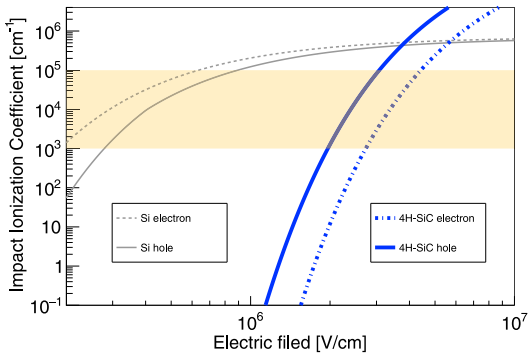

Fig. 1. Impact ionization coefficient of Si and 4H-SiC at T = 300 K, dashed line for electron and solid line for hole. For Si, the van Overstraeten–de Man model [18] is applied, which is validated by LGAD simulation in previous studies [19,20]. The blue lines are from the Hatakeyama model in the ⟨0001⟩ direction of 4H-SiC based on measurements [21]. A possible low gain region for 0.1 ∼ 1.0 μm gain layer is marked by the yellow band.

and lower temperature sensitivity. Additionally, the average rate of electron–hole pair generation resulting from the passage of Minimum Ionization Particles (MIPs) through 4H-SiC material is approximately ∼ 55 pairs/μm [15]. This implies that within a 50 μm thick 4H-SiC LGAD operating with a gain of 10, the signal amount would be around ∼ 4 fC, a value that aligns well with the capabilities of standard readout electronics.

Our group has reported that 4H-SiC detectors have good timing performance for MIP detection. A time resolution of σ_T <100 ps could be achieved in 100 μm 4H-SiC PIN for the detection of MIPs [16]. A corresponding simulation indicates the time resolution σ_T of a 3D 4H-SiC detector could reach ∼25 ps and shows good stability at high temperatures [17]. It is of great interest to design other 4H-SiC structures like LGAD for fast particle detection.

In this work, we designed and simulated two kinds of SiC LGADs for different application requirements, discussed different gain layer thicknesses and doping concentrations, and further studied their leakage currents and capacitances. Otherwise, the gain factor when the same U/V_{BD} as gain efficiency is defined to study the influence for different electric field profiles. Those studies provide guidance for the future production of 4H-SiC detectors.

2. 4H-SiC LGAD design

2.1. Modeling

To detect MIPs in a typical LGAD structure with two active layers: gain layer and bulk layer, the impact ionization coefficient and the generation of e–h pairs are the most essential factors that should be considered in the design of 4H-SiC LGAD. The impact ionization coefficient is related to the thickness and electric field of the gain layer. And the initial e–h pairs is mainly determined by the thickness and doping concentration of the bulk layer. Therefore, the prototype of the 4H-SiC LGAD can be obtained by studying the impact ionization coefficient and e–h pair generation.

Fig. 1 lists the impact ionization coefficients of Si from van Overstraeten–de Man model [18] and 4H-SiC from Hatakeyama model [21]. Based on the previous study of P-type Si-LGAD with a 1 μm thickness gain layer, the electric field ranges from $2 \times 10^5 \sim 3 \times 10^5$ V/cm [20]. And the corresponding impact ionization coefficient of the low gain region is from 10^3 cm^{-1} ∼ 10^5 cm^{-1} as highlighted in the yellow band in Fig. 1. Similarly, for 4H-SiC LGAD with the gain layer (0.1–1 μm), to obtain the same impact ionization coefficient as Si LGAD, the electric field is about $1 \times 10^6 \sim 4 \times 10^6$ V/cm. In terms of 4H-SiC, holes have a greater multiplication rate than electrons, a n type structure is adopted in our work and the impact ionization of initial holes dominates the carrier multiplication.

To effectively detect MIPs, it is essential to generate enough electron–hole pairs in the thick bulk layer to collect enough charges. On the contrary, the generated signal current of a thinner bulk layer exhibits a faster-rising edge compared to a thicker one, which is beneficial to improve the time resolution. Therefore, a medium thickness (50 μm) bulk layer is considered, in which ∼2500 initial e–h pairs could be ionized by MIP. After around 10 times multiplication, approximately 4 fC of charges are collected, which aligns well with the capabilities of standard readout electronics. In addition, to fully deplete the bulk layer under an appropriate voltage, the doping concentration should be as low as possible. Based on our previous study, a high quality 100 μm 4H-SiC epitaxy layer with a doping level $< 1 \times 10^{14}$ cm^{-3} has been achieved successfully in a 4H-SiC PIN device [16]. Conservatively, the doping level of the bulk layer 1×10^{14} cm^{-3} is adopted in this 4H-SiC LGAD design.

To establish a stable space charge region to maintain its operating status, the bias voltage U of LGAD with an appropriate gain should satisfy the condition below:

$$V_{FD} < U < V_{BD} \tag{1}$$

where V_{FD} is the full depletion voltage and V_{BD} is the breakdown voltage. In our design, we require a gain ∼ 10 at U = 500 V and $V_{FD} < \frac{1}{2}V_{BD}$ to guarantee that the operating voltage range could be applied by ordinary source meter with a low power consumption concurrently. Under these conditions, the thickness and doping level of the 4H-SiC LGAD could be deduced analytically.

Taking the LGAD with $p^{++}-n^{+}_{gain}-n^{-}_{bulk}$ doping profile as an example, V_{FD} is calculated by

$$\begin{aligned} V_{FD} =& V_{bulk} + V_{gain} \\ =& \frac{q}{2\varepsilon_{SiC}\varepsilon_0} \times (N^{eff}_{bulk} \times d^2_{bulk} \\ &+ N^{eff}_{gain} \times d^2_{gain} + 2 \times N^{eff}_{bulk} \times d_{gain} \times d_{bulk}) \end{aligned} \tag{2}$$

where q is the unit charge, V_{gain} and V_{bulk} are the depletion voltages of the gain layer and the bulk, N^{eff}_{gain} and N^{eff}_{bulk} are doping levels, d_{gain} and d_{bulk} are the thickness of corresponding layers. V_{bulk} is estimated to be around 230 V if d_{bulk} = 50 μm and $N^{eff}_{bulk} = 1 \times 10^{14}$ cm^{-3}.

The electric field of gain layer E_{gain} could also be derived:

$$E_{gain}(x) = \frac{U - V_{FD}}{d_{bulk} + d_{gain}} + \frac{q}{\varepsilon_{SiC}\varepsilon_0}[N^{eff}_{bulk} \times d_{bulk} + N^{eff}_{gain} \times (d_{gain} - x)] \tag{3}$$

The impact ionization coefficient of electrons α_n and holes α_p could be calculated by different models. Considering the heterogeneity of the 4H-SiC, Hatakeyama model [21] is selected in this work. At room temperature, the model can be expressed as

$$\alpha_{n,p}(x) = a_{n,p}\exp(-\frac{b_{n,p}}{E_{gain}(x)}). \tag{4}$$

where $a_{n,p}$ and $b_{n,p}$ are fitted parameters from Hatakeyama model. Therefore, the quantity of e–h pairs $M(x)$ created by one single initial e–h pair at position x in the depleted gain layer is [22]

$$M(x) = \frac{\exp\left[\int_0^x (\alpha_p - \alpha_n)\, dx\right]}{1 - \int_0^{d_{gain}} \alpha_n \exp\left[\int_0^x (\alpha_p - \alpha_n)\, dx\right] dx} \tag{5}$$

The breakdown condition is assumed to be $Gain = M(d_{gain}) = \infty$.

Consequently, for constant V_{FD} and V_{BD}, an approximate relation between N^{eff}_{gain} and d_{gain} can be determined by Eq. (1)–(5). We calculate the $N^{eff}_{gain} - d_{gain}$ relation for V_{FD} and V_{BD} between 300 V and 700 V. An example of $V_{FD} = V_{BD} = 500\ V$ is shown in Fig. 2, which indicates the available N^{eff}_{gain} and d_{gain} values should be located in the "allowed region" under the black line (Gain = ∞). Some important information could be extracted from Fig. 2 to guide the design of 4H-SiC LGAD:

(1) d_{gain} could not be larger than 1.5 μm. Otherwise, the device will undergo premature breakdown before full depletion.

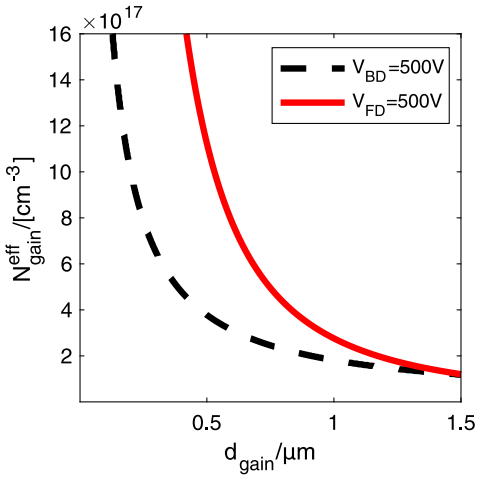

Fig. 2. The relation of N_{gain}^{eff} and d_{gain} under different conditions, 50 μm n bulk layer with 1×10^{14} cm^{-3} doping level when U = 500 V.

Table 1
Two types of 4H-SiC detectors with different structures.

	Layer	Name	Thickness [μm]	Doping [cm^{-3}]
Triangle-Type	p^{++}	contact	0.3	1×10^{19}
	n^{+}	Gain	*	*
	n^{-}	Bulk	50.0	1×10^{14}
	n_{buff}	Buffer	5.0	1×10^{18}
	n^{++}	Substrate	10.0	1×10^{20}
Trapezoid-Type	p^{++}	Contact	0.3	1×10^{19}
	n	Gain	*	1×10^{16}
	n^{+}	Electric field control	0.1	*
	n^{-}	Bulk	50.0	1×10^{14}
	n_{buff}	Buffer	5.0	1×10^{18}
	n^{++}	Substrate	10.0	1×10^{20}

* Study in this work.

(2) In general, N_{gain}^{eff} decreases with the increase of d_{gain} for the same gain efficiency. As d_{gain} increases from 0 to 0.4 μm, N_{gain}^{eff} rapidly decreases by nearly an order of magnitude, and the relationship curve between them gradually flattens after d_{gain} is larger than 0.4 μm. Therefore, $d_{gain} < 0.4$ μm is not suggested due to the high sensitivity of $Gain(d_{gain}, N_{gain}^{eff})$.

(3) The thickness of 1 μm is reasonable, but in the practical process, premature breakdown will be easily caused by fluctuations of N_{gain}^{eff} and d_{gain}.

For a comprehensive consideration, a gain layer with the thickness of 0.5 μm is adopted and its doping concentration (N_{gain}^{eff})is about 4×10^{17} cm^{-3}. In the following simulation (Section 3), varying doping concentrations from 4.07×10^{17} cm^{-3} to 4.13×10^{17} cm^{-3} are used to simulate the electric properties.

2.2. Structure

A typical LGAD structure consists of four layers including $p^{++} - n^{+} - n^{-} - n^{++}$ (see Fig. 3(a)), where p^{++} and n^{++}doped layers contribute to a stable space charge region, and the n^{-} doped layer is the bulk layer which dominates the generation of initial e–h pairs.

As a gain layer, the n^{+} doped layer generates a strong electric field in this region under the reverse bias. Charge carriers can be accelerated in this high electric field, and collide with lattice atoms to ionize the electron–hole pairs. The result is the avalanche multiplication effect, increasing the carrier concentration and greatly improving its detection efficiency.

Because of the "triangle" electric field profile between the p^{++} layer and n^{+} layer, we address the structure shown in Fig. 3(a) as Triangle-Type 4H-SiC LGAD. The parameters of the epitaxial layers are listed in Table 1 where the thickness d_{gain} and doping level N_{gain}^{eff} of the gain layer are studied in this work.

Another structure of $p^{++} - n - n^{+} - n^{-} - n^{++}$ (see Fig. 3(b)) is also considered in this work. To avoid the direct epitaxial growth of p^{++} doped layer on n^{+} doped layer, a n doped layer can be inserted between the above two layers to change the electric field shape of the gain layer region. The n^{+} layer and n layer are equivalent to the gain layer as a whole, and the n^{+} layer is called the electric field control layer.

Similarly, the structure shown in Fig. 3(b) is addressed as Trapezoid-Type 4H-SiC LGAD because of the "trapezoid" electric field profile. Different from the five-layer Triangle-Type, the Trapezoid-Type has an extra electric field control layer which is inserted between the gain layer and the bulk layer. Profiles of each layer are listed in Table 1 where the thickness d_{gain} of gain layer and doping level N_{ec}^{eff} of field control layer are studied in this work.

In addition to the above two LGADs, a 4H-SiC PIN detector (50 μm) without the gain layer is designed for comparative study. Considering the horizontal diffusion of carriers in the process of MIP injection, its width is fixed to 10 μm in 2D simulation.

3. Simulation

In order to further specify the doping level of the gain layer, the characteristics of 4H-SiC LGAD for different designs are simulated using TCAD (Technology Computer Aided Design) tools.

3.1. Physical parameters in TCAD simulation

The physical parameters used in this work for TCAD simulation are listed below: The dielectric constant of 4H-SiC is $\varepsilon_{SiC} = 9.7$; The electron and hole effective mass and conduction band density-of-state models are taken from [23]; Parameters of carrier mobility model with doping-dependence refer to [24,25] which is fitted from measured data; Hatakeyama model is selected as the impact ionization model [21] and it has been applied to device simulation with anisotropic features [26]; The MIPs is simulated by the heavy ion model of TCAD [27] where the ionization rate is 55 e–h pairs/μm; The wafer system of 4H-SiC with a 4° miscut angle is used in all simulations.

3.2. I-V and $1/C^2$-V profiles

To determine the depletion voltage of gain layer V_{GL} and full depletion voltage V_{FD} of the Triangle-Type 4H-SiC LGAD, $1/C^2$-V relations are calculated.

As shown in Fig. 4(a), the influence of fluctuation of N_{gain}^{eff} to V_{GL} could be neglected and the V_{FD} of different 4H-SiC designs with different N_{gain}^{eff} ($4.07 \sim 4.13 \times 10^{17}$ cm^{-3}) are smaller than 500 V. The I-V curves imply the breakdown voltage V_{BD} of the Triangle Type 4H-SiC LGAD is negatively correlated with the doping concentration of the gain layer, shown in Fig. 4(b). Fig. 4(c) shows the relationship between N_{gain}^{eff} and V_{BD} at different gain thickness ranging from 0.1 μm to 1 μm. Considering the influence of d_{gain}, the order of magnitude of N_{gain}^{eff} is about 10^{18} cm^{-3} when d_{gain} is 0.1 μm and about 10^{17} cm^{-3} when d_{gain} is 1.0 μm. These results agree with the prediction of the analysis in Fig. 2.

To obtain a flat electric field profile and control the electric field near the gain layer, Trapezoid-Type 4H-SiC LGAD is introduced (see Fig. 3(b)). Similarly, the $1/C^2$-V and I-V curves are simulated for Trapezoid-Type 4H-SiC LGAD (see Figs. 4(d) and 4(e)). Similar to the Triangle-Type 4H-SiC LGAD, the N_{ec}^{eff} of the electric field control layer (n^{+}) of the Trapezoid-Type LGAD has little influence on the V_{FD}. The breakdown voltage (V_{BD}) is restrained to 500 V–1000 V. However, the V_{BD} of Trapezoid-Type 4H SiC LGAD is more sensitive to the effective

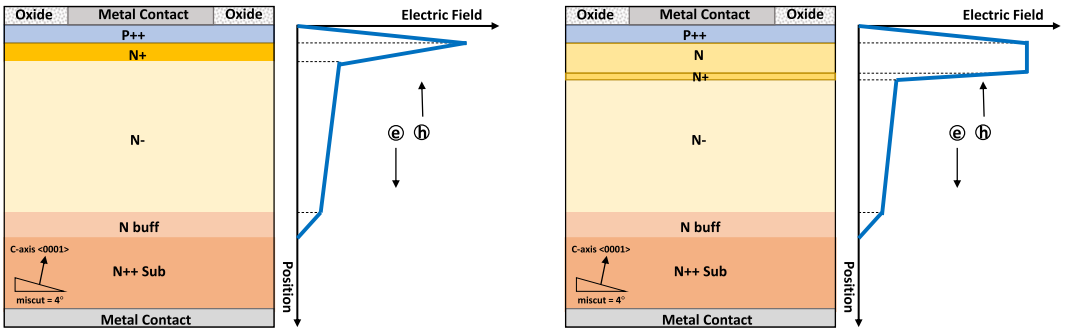

Fig. 3. Longitudinal layers design of the 4H-SiC LGAD studied in this work. (a) "Triangle" electric field. (b) "Trapezoid" electric field.

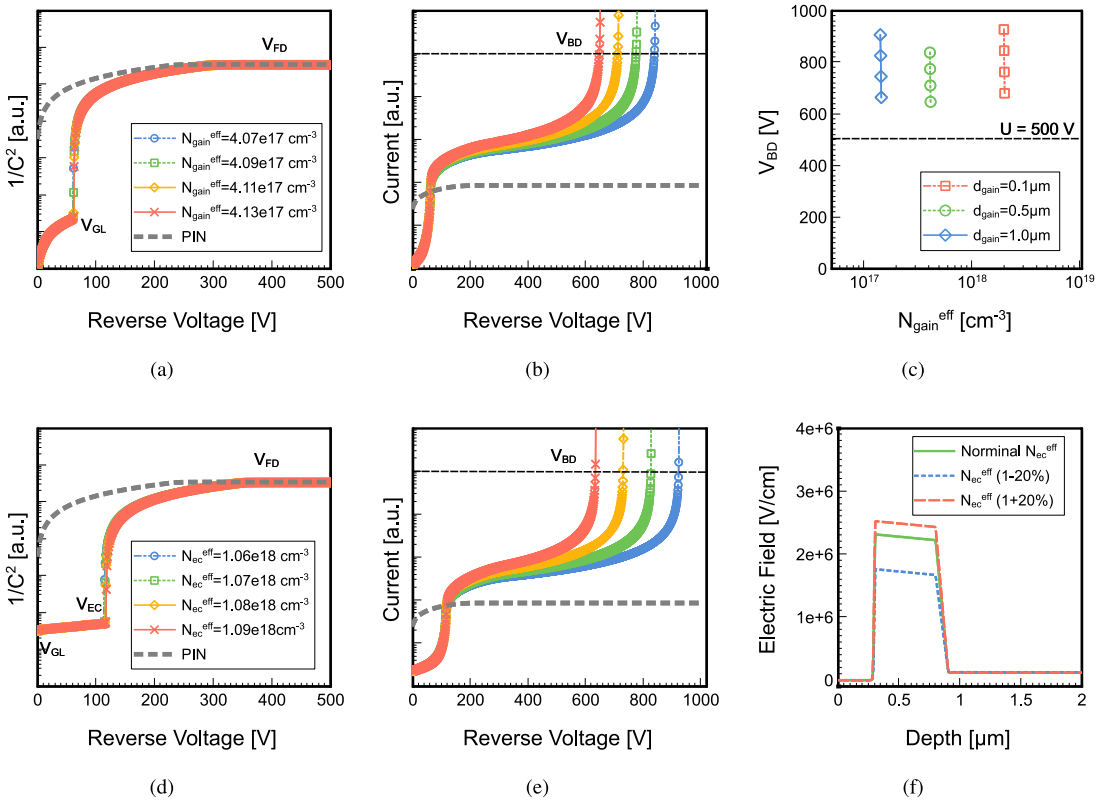

Fig. 4. Simulated results for 4H-SiC LGAD with $d_{gain} = 0.5$ μm. (a)(b) $1/C^2 - V$ and $I - V$ relations of Triangle-Type. (c) $V_{BD} - N_{gain}^{eff}$ relations of different d_{gain}. (d)(e) $1/C^2 - V$ and $I - V$ relations of Trapezoid-Type. (f) Electric field in the gain layer of Trapezoid-Type when N_{ec}^{eff} changed ±20%. For (a)(b)(d)(e) the colored lines are for 4H-SiC LGADs and the dotted gray lines are for PIN.

doping concentration of the field control layer compared with the $V_{BD} - N_{ec}^{eff}$ of the Triangle-Type.

Fig. 4(f) demonstrates the control effect to the electric field when the effective doping level of the control layer N_{ec}^{eff} changed ±20%. When the electric field is approximately 2.3×10^6 V/cm, a gain factor about 10 can be achieved in the 4H-SiC LGAD with $d_{gain} = 0.5$ μm.

As shown in Figs. 4(b) and 4(e), when $U < V_{GL}$, the depletion area volume of 4H SiC LGAD is very small, so its leakage current is less than that of PIN. As the voltage increases, the depletion region increases gradually, and its leakage current increases rapidly and is far greater than that of PIN. The gain of leakage current is ∼ 10, which indicates that a low gain is achieved.

3.3. Simulation of MIP detection

Apart from electrical properties, as a particle detector, one of the most valuable indicators of the LGAD are the gain factor. To determine the gain factor when MIPs pass through 4H-SiC LGAD, we use a heavy ion model in TCAD with the same e–h pair generation rate as MIP, which is defined as:

$$Gain = \frac{Q_{LGAD}}{Q_{PIN}} = \frac{\int_0^T i(t)_{LGAD}}{\int_0^T i(t)_{PIN}} \tag{6}$$

where Q is the collected charge, $i(t)$ is the stimulated current by MIP and T is the time period for collection.

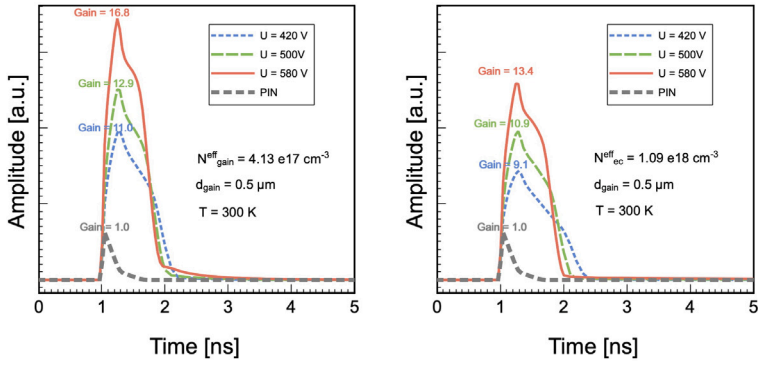

(a) (b)

Fig. 5. Stimulated current by MIP in (a) Triangle-Type and (b) Trapezoid-Type 4H-SiC LGADs under different operating voltages. Gray lines are for PIN at U = 500 V.

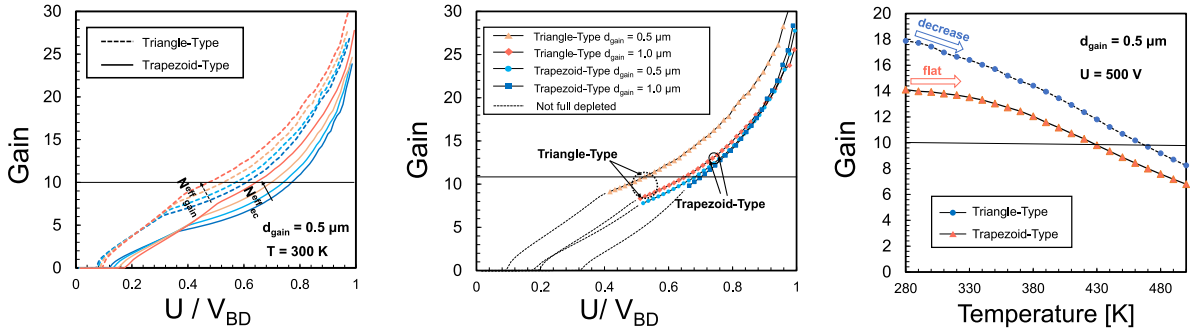

(a) (b) (c)

Fig. 6. (a) Relations between gain and U/V_{BD} for Triangle-Type 4H-SiC LGAD (dotted lines) and Trapezoid-Type 4H-SiC LGAD (solid lines). Colored lines represent different doping levels. (b) Relations between gain and U/V_{BD} for different thicknesses of the gain layer. The dotted lines are for Triangle-Type and the solid lines are for Trapezoid-Type. (c) The gain factor under operating voltage U = 500 V at temperatures from T = 300 K to T = 500 K.

Figs. 5(a) and 5(b) demonstrate the current stimulated by MIPs under different operating voltages. Compared with the simulated current of PIN, the current gain for both types of 4H-SiC LGAD is greater than 10 when U = 500 V. Under the same operating voltage, the gain of Triangle-Type is higher than that of Trapezoid-Type. This could be interpreted by a higher electric field peak of the "triangle" electric field profile. Based on the simulation, we determine that the electric fields of Triangle Type and Trapezoid type are 3.2×10^6 V/cm and 2.3×10^6 V/cm respectively, to establish a 4H-SiC LGAD with $d_{gain} = 0.5$ µm.

3.4. Gain efficiency and stability

To compare the gain efficiency for two types 4H-SiC LGAD, the relations between gain and U/V_{BD} are studied, see Fig. 6(a). The higher gain factor under the same U/V_{BD} means higher gain efficiency. The gain factor increases slightly with increasing N^{eff}_{gain} or N^{eff}_{ec}. The electric field profile dominates the gain efficiency. The Triangle-Type 4H-SiC LGAD has higher gain efficiency because it has a higher gain factor than Trapezoid-Type at the same U/V_{BD} value. However, it also indicates that when U/V_{BD} is larger than 0.8, it is easier to reach the breakdown threshold with the steep increase in the gain of the Triangle-Type 4H-SiC LGAD.

It is worth noting that the Trapezoid-Type 4H-SiC LGAD behaves more stable, shown as Fig. 6(b). When the thickness of the gain layer increases from 0.5 µm to 1.0 µm, the gain factors of Trapezoid-Type 4H-SiC LGAD change little. This means the gain efficiency does not rely on d_{gain}. On the other hand, for the Triangle-Type 4H-SiC LGAD, an increase in d_{gain} at a constant value of U/V_{BD} leads to a decrease in the gain factor. This phenomenon suggests that a thinner gain layer correlates with higher gain efficiency, albeit at the expense of hastening the breakdown of the device. Therefore, Trapezoid-Type 4H-SiC LGAD is better if one considers its stability.

To investigate temperature dependence and potential application in high-temperature environments, gain factors are simulated under the temperature ranging from 300 K to 500 K, shown as Fig. 6(c). Under the same operating voltage, the gain factor decreases with increasing temperature. It is interpreted by the decrease in the impact ionization coefficient predicted by the Hatakeyama model [21]. The gains of both types are greater than 10 when the temperature is below 400 K. When the temperature is up to 500 K, the gain factors of both types are still bigger than 5. This indicates the 4H-SiC LGAD has a good performance in high-temperature environments. A potential indication is shown in Fig. 6(c) that the gain of Trapezoid-Type 4H-SiC LGAD decreases gently compared with Triangle-Type 4H-SiC LGAD.

4. Summary

Promoted by the benefits of SiC material, we propose to design a 4H-SiC LGAD for MIP detection in high radiation and high-temperature environment. Based on the analysis, we provide a guideline to determine the doping level and thickness of the gain layer in 4H-SiC LGAD. Triangle-Type and Trapezoid-Type LGAD structures with different electric profiles are designed for MIPs detection. In our work, $d_{gain} = 0.5$ µm with $E \sim 2.3\times10^6$ V/cm is adopted which has a 50 µm, 1×10^{14} cm^{-3} bulk layer. In the simulation, a gain > 10 is achieved when the operating voltage U is between V_{FD} and V_{BD}. We define the gain factor under the same U/V_{BD} ratio to describe the gain efficiency. Compared with the effective doping level of the gain layer, the electric field profile

dominates the gain efficiency. A Triangle-Type LGAD has higher gain, while Trapezoid-Type shows high stability and robustness.

According to the above study, we will develop the corresponding 4H-SiC LGAD devices for the requirements of MIPs detection. More interesting results will be obtained for practical devices and help us to understand the impact ionization in the 4H-SiC, especially 4H-SiC LGAD structure.

Declaration of competing interest

The authors declare that they have no known competing financial interests or personal relationships that could have appeared to influence the work reported in this paper.

Data availability

Data will be made available on request.

Acknowledgment

This work has been supported by the National Natural Science Foundation of China (No. 11961141014 and No. 12205321), the State Key Laboratory of Particle Detection and Electronics, China (No. SKLPDE-ZZ-202218) under CERN RD50 Collaboration framework.

References

[1] ATLAS Collaboration, Technical Design Report for the ATLAS Inner Tracker Strip Detector, Technical report, CERN, Geneva, 2021, URL https://cds.cern.ch/record/2257755.

[2] V. Sola, et al., Ultra-fast silicon detectors for 4D tracking, J. Instrum. 12 (02) (2017) http://dx.doi.org/10.1088/1748-0221/12/02/c02072.

[3] G. Pellegrini, et al., Technology developments and first measurements of Low Gain Avalanche Detectors (LGAD) for high energy physics applications, Nucl. Instrum. Methods A 765 (2014) http://dx.doi.org/10.1016/j.nima.2014.06.008, doi: DOI: 10.1016/j.nima.2014.06.00810.1016/j.nima.2014.06.008.

[4] H.F.W. Sadrozinski, et al., 4D tracking with ultra-fast silicon detectors, Rep. Progr. Phys. 81 (2) (2018) http://dx.doi.org/10.1088/1361-6633/aa94d3.

[5] V. Sola, et al., First FBK production of 50 um ultra-fast silicon detectors, Nucl. Instrum. Methods A 924 (2019) http://dx.doi.org/10.1016/j.nima.2018.07.060.

[6] G. Giacomini, et al., Development of a technology for the fabrication of Low-Gain Avalanche Diodes at BNL, Nucl. Instrum. Methods A 934 (2019) http://dx.doi.org/10.1016/j.nima.2019.04.073.

[7] K. Wu, et al., Design of low gain avalanche detectors (LGAD) with 400 keV ion implantation energy for multiplication layer fabrication, Nucl. Instrum. Methods A 984 (2020) http://dx.doi.org/10.1016/j.nima.2020.164558.

[8] Y. Fan, et al., Radiation hardness of the low gain avalanche diodes developed by NDL and IHEP in China, Nucl. Instrum. Methods A 984 (2020) http://dx.doi.org/10.1016/j.nima.2020.164608.

[9] S. Xiao, et al., Beam test results of NDL low gain avalanche detectors (LGAD), Nucl. Instrum. Methods A 989 (2021) http://dx.doi.org/10.1016/j.nima.2020.164956.

[10] Y. Yang, et al., Characterization of the first prototype NDL Low Gain Avalanche Detectors (LGAD), Nucl. Instrum. Methods A 1011 (2021) http://dx.doi.org/10.1016/j.nima.2021.165591.

[11] Y. Tan, et al., Radiation effects on NDL prototype LGAD sensors after proton irradiation, Nucl. Instrum. Methods A 1010 (2021) http://dx.doi.org/10.1016/j.nima.2021.165559.

[12] G. Kramberger, et al., Radiation effects in Low Gain Avalanche Detectors after hadronirradiations, J. Instrum. 10 (07) (2015) http://dx.doi.org/10.1088/1748-0221/10/07/p07006.

[13] M. Ferrero, et al., Radiation resistant LGAD design, Nucl. Instrum. Methods A 919 (2019) http://dx.doi.org/10.1016/j.nima.2018.11.121.

[14] J.M. Rafí, et al., Electron, neutron, and proton irradiation effects on SiC radiation detectors, IEEE Trans. Nucl. Sci. 67 (12) (2020) 2481–2489, http://dx.doi.org/10.1109/TNS.2020.3029730.

[15] F. Moscatelli, et al., Measurements and simulations of charge collection efficiency of p+/n junction SiC detectors, Nucl. Instrum. Methods A 546 (1) (2005) 218–221, Proceedings of the 6th International Workshop on Radiation Imaging Detectors.

[16] T. Yang, et al., Time resolution of the 4H-SiC PIN detector, Front. Phys. 10 (2022) http://dx.doi.org/10.3389/fphy.2022.718071.

[17] Y. Tan, et al., Timing performance simulation for 3D 4h-SiC detector, Micromachines 13 (1) (2022) http://dx.doi.org/10.3390/mi13010046.

[18] R. Van Overstraeten, et al., Measurement of the ionization rates in diffused silicon p-n junctions, Solid-State Electron. 13 (5) (1970) http://dx.doi.org/10.1016/0038-1101(70)90139-5.

[19] M. Mandurrino, et al., Analysis and numerical design of resistive AC-coupled silicon detectors (RSD) for 4D particle tracking, Nucl. Instrum. Methods A 959 (2020) http://dx.doi.org/10.1016/j.nima.2020.163479.

[20] T. Yang, et al., Leakage current simulations of Low Gain Avalanche Diode with improved radiation damage modeling, Nucl. Instrum. Methods A 1040 (2022) 167111, http://dx.doi.org/10.1016/j.nima.2022.167111.

[21] T. Hatakeyama, et al., Impact ionization coefficients of 4H silicon carbide, Appl. Phys. Lett. 85 (8) (2004) http://dx.doi.org/10.1063/1.1784520.

[22] B.J. Baliga, Fundamentals of Power Semiconductor Devices, 2019, http://dx.doi.org/10.1007/978-3-319-93988-9.

[23] G. Wellenhofer, U. Rössler, Global band structure and near-band edge states, Physica Status Solidi 202 (1) (1997) 107–123, http://dx.doi.org/10.1002/1521-3951.

[24] W.J. Schaffer, et al., Conductivity anisotropy in epitaxial 6H and 4H SiC, MRS Online Proceeding Libr. Arch. 339 (1994) http://dx.doi.org/10.1557/PROC-339-595.

[25] T. Ayalew, SiC Semiconductor Devices, Technology, Modeling, and Simulation (Ph.D. thesis), Technishen Universiaet Wien, Austria, 2004.

[26] T. Hatakeyama, Measurements of impact ionization coefficients of electrons and holes in 4H-SiC and their application to device simulation, Physica Status Solidi (a) 206 (10) (2009) 2284–2294, http://dx.doi.org/10.1002/pssa.200925213.

[27] Sentaurus Manual, https://www.synopsys.com.